ELSEVIER

Astroparticle Physics 4 (1995) 33–43

Astroparticle Physics

Performance of the MACRO streamer tube system in the search for magnetic monopoles

The MACRO Collaboration

M. Ambrosio[f], R. Antolini[g], G. Auriemma[n,1], R. Baker[k], A. Baldini[m], G.C. Barbarino[ℓ], B.C. Barish[d], G. Battistoni[f,2], R. Bellotti[a], C. Bemporad[m], P. Bernardini[j], H. Bilokon[f], V. Bisi[p], C. Bloise[f], C. Bower[h], S. Bussino[n], F. Cafagna[a], M. Calicchio[a], D. Campana[ℓ], M. Carboni[f], M. Castellano[a], S. Cecchini[b,3], F. Cei[m,4], V. Chiarella[f], A. Corona[n], S. Coutu[k], G. De Cataldo[a], H. Dekhissi[b,5], C. De Marzo[a], I. De Mitri[i], M. De Vincenzi[n,6], A. Di Credico[g,n], O. Erriquez[a], C. Favuzzi[a], C. Forti[f], P. Fusco[a], G. Giacomelli[b], G. Giannini[m,7], N. Giglietto[a], M. Goretti[n], M. Grassi[m], A. Grillo[g], F. Guarino[f], P. Guarnaccia[a], C. Gustavino[g], A. Habig[h], K. Hanson[k], A. Hawthorne[h], R. Heinz[h], J.T. Hong[c], E. Iarocci[f,8], E. Katsavounidis[d], E. Kearns[c], S. Kyriazopoulou[d], E. Lamanna[n], C. Lane[e], D.S. Levin[k], P. Lipari[n], R. Liu[d], N.P. Longley[d], M.J. Longo[k], Y. Lu[o], G. Ludlam[c], G. Mancarella[j], G. Mandrioli[b], A. Margiotta-Neri[b], A. Marini[f], D. Martello[j], A. Marzari-Chiesa[p], M.N. Mazziotta[a], D.G. Michael[d], S. Mikheyev[g,9], L. Miller[h], M. Mittelbrunn[c], P. Monacelli[i], T. Montaruli[a], M. Monteno[p], S. Mufson[h], J. Musser[h], D. Nicoló[m,4], R. Nolty[d], C. Okada[c], C. Orth[c], G. Osteria[ℓ], O. Palamara[j], S. Parlati[g], V. Patera[f,8], L. Patrizii[b], R. Pazzi[m], C.W. Peck[d], S. Petrera[j], N.D. Pignatano[d], P. Pistilli[j], V. Popa[b,10], A. Rainó[a], J. Reynoldson[g], F. Ronga[f], U. Rubizzo[ℓ], A. Sanzgiri[o], F. Sartogo[n], C. Satriano[n,1], L. Satta[f,8], E. Scapparone[b], K. Scholberg[d], A. Sciubba[f,8], P. Serra-Lugaresi[b], M. Severi[n], M. Sitta[p], P. Spinelli[a], M. Spinetti[f], M. Spurio[b], R. Steinberg[e], J.L. Stone[c], L.R. Sulak[c], A. Surdo[j], G. Tarlé[k], F. Tassoni[n], V. Togo[b], V. Valente[f], C.W. Walter[d], R. Webb[o]

[a] *Dipartimento di Fisica dell'Università di Bari and INFN, 70126 Bari, Italy*
[b] *Dipartimento di Fisica dell'Università di Bologna and INFN, 40126 Bologna, Italy*
[c] *Physics Department, Boston University, Boston, MA 02215, USA*
[d] *California Institute of Technology, Pasadena, CA 91125, USA*
[e] *Department of Physics and Atmospheric Science, Drexel University, Philadelphia, PA 19104, USA*
[f] *Laboratori Nazionali di Frascati dell'INFN, 00044 Frascati (Roma), Italy*
[g] *Laboratori Nazionali del Gran Sasso dell'INFN, 67010 Assergi (L'Aquila), Italy*
[h] *Depts. of Physics and of Astronomy, Indiana University, Bloomington, IN 47405, USA*
[i] *Dipartimento di Fisica dell'Università dell'Aquila and INFN, 67100 L'Aquila, Italy*
[j] *Dipartimento di Fisica dell'Università di Lecce and INFN, 73100 Lecce, Italy*
[k] *Department of Physics, University of Michigan, Ann Arbor, MI 48109, USA*
[ℓ] *Dipartimento di Fisica dell'Università di Napoli and INFN, 80125 Napoli, Italy*

SSDI 0927-6505(95)00023-2

[a] Dipartimento di Fisica dell'Università di Pisa and INFN, 56010 Pisa, Italy
[n] Dipartimento di Fisica dell'Università di Roma "La Sapienza" and INFN, 00185 Roma, Italy
[o] Physics Department, Texas A&M University, College Station, TX 77843, USA
[p] Dipartimento di Fisica Sperimentale dell'Università di Torino and INFN, 10125 Torino, Italy

Received 7 April 1995

Abstract

We describe the techniques chosen to search for magnetic monopoles using the MACRO streamer tube sub-system. The hardware and the details of the analysis procedures will be discussed also. The results for slowly moving monopoles are reported from a first data taking period using only part of the detector.

1. Introduction

The MACRO experiment at the Gran Sasso Laboratory is a large acceptance ($\sim$ 10000 m^2 sr) underground detector devoted mainly to the search for super-massive magnetic monopoles predicted by most GUT theories. In a few years' running this detector will have the sensitivity to a GUT monopole flux one order of magnitude beyond the Parker bound [1] for monopole velocities greater than 10^{-4} c.

In order to obtain a reliable interpretation of candidate events, redundancy and complementarity are required. This is accomplished by the use of three different detection techniques: streamer tubes, scintillation counters and track-etch plastics. Streamer and scintillation detectors independently trigger the readout of both sub-systems. Furthermore, the analysis procedures can be kept separate until candidates selection.

The result of a first monopole analysis performed with the MACRO scintillator sub-system is reported in Ref. [2]. In this paper we describe the capabilities of the MACRO streamer tube sub-system in the search for GUT monopoles. The results of the analysis of a first sample of data in the beta range $10^{-4} < \beta < 5 \times 10^{-3}$ are reported.

2. Hardware configuration

MACRO consists of six "supermodules" with total dimension $77 \times 12 \times 9$ m^3 (Fig. 1). Each supermodule is divided into a lower and an upper part. A detailed description of the lower part of the first supermodule is given in Ref. [3]. Each supermodule consists of two separate modules made of ten horizontal streamer tube planes (6×12 m^2) interleaved with seven rock absorber planes, two scintillation counter planes (on the top and bottom) and one track-etch plastic plane in the middle. The east and west sides (12×5 m^2) of each lower supermodule are closed by a sandwich of two sets of vertical streamer tube planes (three layers each), interleaved with a scintillation counter plane. Two other "vertical detector systems" close the north and south walls. Each vertical plane is divided into seven segments.

The upper part of each supermodule consists of two vertical detector systems and of a roof made of two sets of two horizontal streamer tube planes (12×12 m^2), interleaved with a scintillation counter plane, without any absorber.

2.1. The streamer tube system

The basic element of each streamer tube plane is an eight-wire chamber (3.2 cm $\times$ 25 cm $\times$ 12 m). Each

[1] Also Università della Basilicata, 85100 Potenza, Italy.
[2] Also INFN Milano, 20133 Milano, Italy.
[3] Also Istituto TESRE/CNR, 40129 Bologna, Italy.
[4] Also Scuola Normale Superiore di Pisa, 56010 Pisa, Italy.
[5] Also Faculty of Sciences, University Mohamed I, B.P. 424 Oujda, Morocco.
[6] Also Dipartimento di Fisica, Università di Roma III, Roma, Italy.
[7] Also Università di Trieste and INFN, 34100 Trieste, Italy.
[8] Also Dipartimento di Energetica, Università di Roma, 00185 Roma, Italy.
[9] Also Institute for Nuclear Research, Russian Academy of Science, 117312 Moscow, Russia.
[10] Also Institute for Atomic Physics, 76900 Bucharest, Romania.

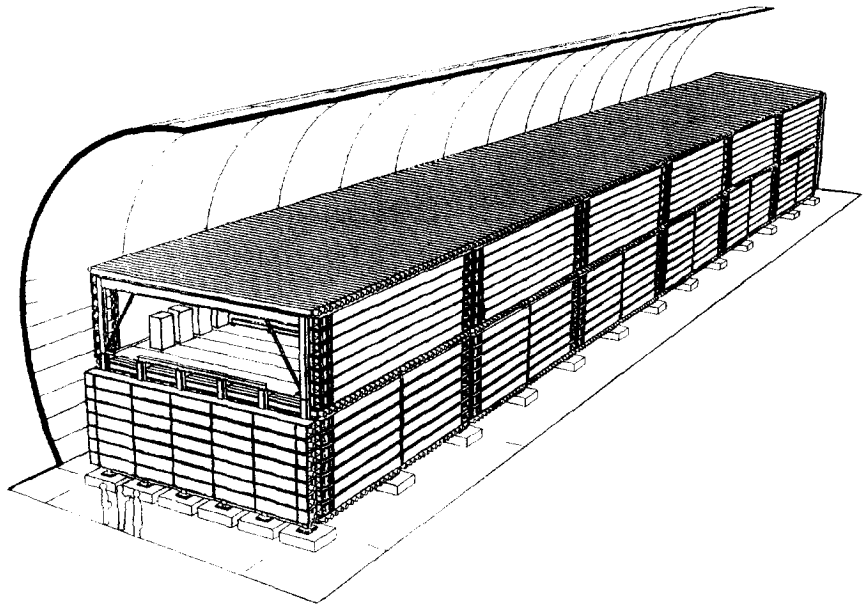

Fig. 1. Pictorial view of the MACRO detector at Gran Sasso.

individual channel is made of a 2.9×2.7 cm^2 cell having three sides coated with low-resistivity graphite and a 100 μm anodic wire. The horizontal streamer tube planes are equipped with a system of pick-up strips at an angle of 26.5° with respect to the wires. The vertical planes of the upper part of MACRO are also equipped with strips at 90° with respect to the wires. Both the strips and anode wires are read out to provide two dimensional coordinates.

The tubes are filled with a 73% He–27% n-pentane gas mixture and are operated in the limited streamer mode.

The tracking efficiency has been measured using cosmic ray muons. In these measurements the few percent inefficiencies that are observed are primarily due to geometrical effects caused by dead spaces between the cells. The cell dimensions and the drift inside a tube produce a time jitter with an approximately triangular shape with a base width of 600 ns, which corresponds to a time resolution of about 140 ns [4].

Helium is used to exploit the Drell effect [5]: the passage of a monopole with $\beta \geq 1.1 \times 10^{-4}$ through a helium atom leaves it in a excited metastable state. The n-pentane can then be ionized by collisions with excited helium atoms (Penning effect). The high cross section for the processes ensures 100% efficiency in detecting bare monopoles with this gas mixture. As shown in Ref. [6], MACRO streamer tubes have high efficiency for single electrons, allowing monopole detection even if the Drell cross section is reduced for monopoles that have captured atomic nuclei [7].

In the higher velocity region ($\beta > 10^{-3}$), where the assumptions used in the Drell calculation do not apply, the standard ionization mechanism for charged particles ensures an energy release several orders of magnitude higher than that due to minimum ionizing particles. In the MACRO streamer tubes, the charge collected on the wires has a logarithmic dependence on the energy released inside the active cell [8], so that a charge measurement allows one to distinguish between monopoles and muons.

These features allow the detection of magnetic monopoles with $\beta > 10^{-4}$.

2.2. *Streamer tube readout*

Streamer tube electronics were designed to be effective in the search for slow particles. In particular the memory depth of each element is large enough to store signals from monopoles crossing the apparatus with any trajectory for β down to 10^{-4}.

Signals from the wires are processed by front-end

boards (eight channels each), producing an analog sum for charge and time measurements. For the horizontal planes, the analog outputs of four adjacent boards (corresponding to 1 m of tubes) are summed and transmitted to the charge and time processor (QTP) [9]; for the vertical planes, the analog sum of two adjacent boards, corresponding to the 50 cm of one vertical segment, is sent to the QTP. The QTP system acts as a 640 μs memory during which the arrival time, width and charge of the streamer pulse are recorded. The charge integration gate is 300 ns long and is stretched for wider signals. Charge resolution is $\sim 5\%$ of the typical charge produced by one minimum ionizing particle and the dynamic range allows measurement of charges 50 times higher. The time resolution of 150 ns is comparable to the intrinsic time jitter of the streamer tubes.

In order to measure spatial coordinates, the signal from each wire is also discriminated and shaped at 550 μs before being sent to parallel-in/serial-out shift register chains. Each chain collects signals from one entire horizontal or vertical plane. These chains are fed into the Streamer Tube Acquisition System (STAS) readout processors [10] which decode the serial information and carry out zero suppression on the raw data. The strip system is read in a similar way: front-end electronics provide signals shaped at 580 μs that are fed into the STAS processors. Both wire and strip signals are also shaped independently at 10 μs and 14 μs respectively to form similar readout chains for the study of fast particles.

2.3. *The streamer tube monopole trigger*

The only assumption made in the trigger design is that a heavy monopole crosses the apparatus without any apparent variation of direction or speed. This loose requirement allows the trigger logic to be sensitive to any massive particle able to produce signals in the streamer tubes.

The streamer trigger consists of two independent sub-systems. One handles the horizontal planes of streamer tubes and the other the vertical planes. The horizontal trigger is composed of eleven circuits: there is a trigger circuit for each supermodule; to avoid losses in the acceptance, five other circuits process the signals coming from the twelve meter regions centered on the boundary between neighboring supermodules. The vertical trigger consists of 26 circuits, one for each vertical streamer system. Monte Carlo computations show that for an isotropic flux of incoming particles the two systems are basically complementary and provide a high acceptance trigger (see Table 1).

Particular attention has been paid to the possibility that monopoles may catalyze nucleon decay [11]. In that case it is possible that fast particles from a nucleon decay may cause dead time in the apparatus before a monopole could cross the entire detector and thus generate a slow particle trigger. To avoid this effect the start of the acquisition is delayed when a fast particle is detected to allow the monopole to exit from the apparatus.

Horizontal trigger. The primary function of the horizontal trigger is to measure the time-of-flight of particles in the range $3 \times 10^{-5} \leq \beta \leq 1$ and distinguish them from the random noise. A complete description is given in Ref. [12].

The wire signals, shaped at 10 μs, are used to produce a unique signal (a digital OR) from each horizontal plane of one module. These ten signals as well as the corresponding signals from the next module are fed to a horizontal trigger unit. The horizontal trigger unit acts as 320 delayed coincidences (β-slices) obtained by means of shift register chains driven by a 1 MHz clock. The β-slice values represent the time-of-flight (ToF) from the height of plane 10 to that of plane 1, measured with a resolution of 3 μs. They are labelled by numbers from -160 to -1 for upward going particles and from 1 to 160 for downward going particles; fired β-slices are recorded when a trigger occurs. As an example, every muon fires the β-slices $+1$ and -1 because of the time resolution of the trigger circuit.

A search is performed every clock cycle (1 μs) among the β-slices for at least one time alignment of a number greater than a preselected value of active planes. In order to avoid any inefficiency due to the 1 μs quantization and to the jitter inside the tubes, most β-slices have a time acceptance greater than the minimum needed. As an example, Fig. 2 shows that the number of 1 μs cells of the seventh β-slice on planes 4, 5, 8 and 9 is higher than the corresponding number of cells for the first β-slice. This produces an increase in the trigger rate by a factor ~ 3 as expected from a computation which takes into account the de-

Table 1
Acceptance values take into account the trigger requirements and the complete geometry of the apparatus. It should be noted that the two trigger sub-systems are almost completely independent.

Acceptance			
Horizontal trigger	Vertical trigger	Total	Full sensitive
≥ 7 planes : H	≥ 4 planes : V	H.OR.V	Box
4250 m^2sr	5030 m^2sr	8280 m^2sr	11000 m^2sr

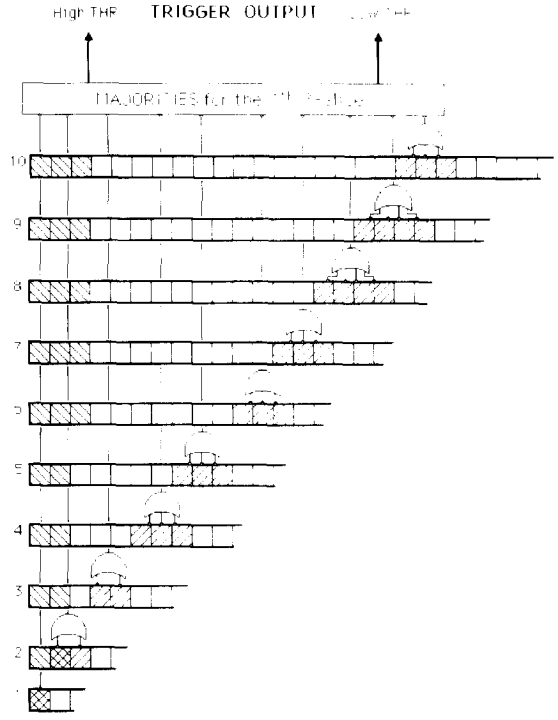

Fig. 2. A simplified scheme of the first β-slices is reported for downgoing particles. Each shift register chain uses the signals coming from a 12×12 m^2 plane. The parallel outputs of several shift register cells are OR-ed and sent to two majority logics that activate the trigger outputs for the low and high thresholds. As an example, the cells that constitute the first and the seventh β-slices are represented with different dashes.

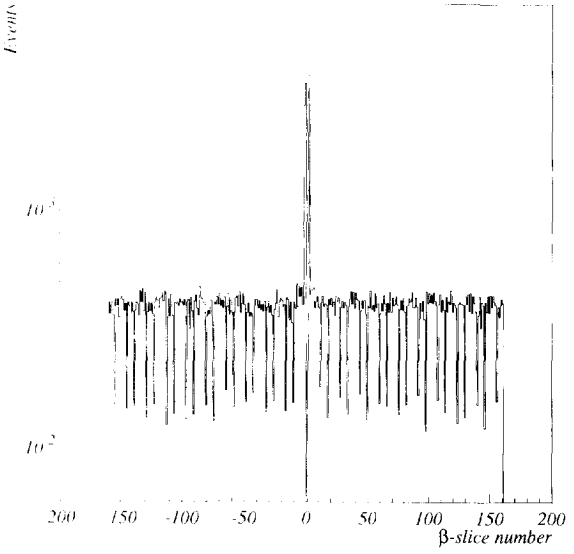

Fig. 3. β-slice frequency distribution for events firing at least seven planes aligned in at least one slice different from +1 and −1. The central peak is due to the effect of the background on the muon ToF measurement. The periodic structure, showing the expected increase in the counting rate by a factor 3 above the full efficiency level, reflects the hardware β-slice definition.

tails of the trigger circuits and the measured counting rate from each plane. This is shown in Fig. 3 where the observed β-slice distribution for a sample of data obtained requiring at least seven fired planes is reported. The periodic structure is due to the fact that every trigger circuit is made of 20 identical gate arrays containing 16 β-slices each.

Each trigger circuit has two outputs. The first appears when at least seven planes are fired, starting the readout of the streamer tubes. The total rate of this trigger is some tenths of hertz, mainly due to the muon background. The second output appears when at least eight planes are fired with a ToF greater than 3 μs and is used to start the acquisition of the scintillator wave form digitizers. These additional requirements reduce the rate of this output by approximately a factor of 100.

Vertical trigger. Each vertical trigger unit processes the signals from a vertical streamer sub-system. The analog sum of the outputs of two adjacent boards of a vertical segment are discriminated by the QTP system and sent to the trigger logic. At least four out of six

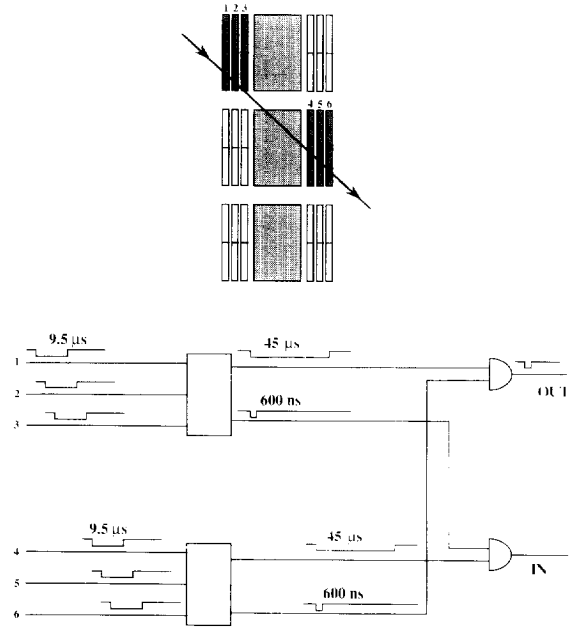

Fig. 4. A particle exiting MACRO (from left to right in the figure) as detected by the vertical trigger. Six roughly aligned pairs of streamer chambers are interested. The timing of the signals is schematically reported: if the crossing time between the inner and outer planes is greater than 600 ns the circuit recognizes the particle direction.

planes are required to be active and aligned (Fig. 4) in a 45 μs time window which is appropriate for particles with $\beta = 10^{-4}$. Furthermore, two 9.5 μs coincidences are separately required for signals coming from the inner and outer planes. In this way the trigger rate caused by radioactivity induced noise is reduced to a tolerable level (a few millihertz).

If the time of flight between inner and outer planes is greater than 600 ns, it is also possible to discriminate between particles entering or leaving the apparatus and to produce the corresponding two trigger outputs. Otherwise, a fast particle trigger signal is produced. Every time a unit generates a trigger, internal registers record the pattern of fired segments.

The vertical trigger system also has a second threshold: if an alignment compatible with that of a slow particle is found in at least five planes, the scintillator waveform digitizers are also read out.

3. Analysis strategies

The streamer tubes time resolution allows identification of slow particles by measuring their time of flight across the apparatus. However, because of time jitter and afterpulsing in the streamer tubes, with this technique particles faster than $5 \times 10^{-3}\, c$ could be confused with cosmic ray muons; hence different analysis strategies must be adopted in the two velocity ranges. The fast analysis is mainly based on the high energy losses of fast monopoles, which result in high charge produced in the streamer developement.

In the case of slow particles, since horizontal and vertical planes act independently and have different monopole trigger logics, two different analyses are carried out.

In the present paper we do not consider monopole-induced nucleon decay; this analysis applies then to a catalysis cross section smaller than a few millibarn. A full Monte Carlo simulation is in progress in order to estimate the detection efficiency as a function of the catalysis cross section, decay modes and branching ratios.

3.1. Horizontal trigger: slow particles

The trigger logic selects events which exhibit a z versus time alignment (expected from a constant speed particle) of at least seven streamer tube hits in one or more of the 320 β-slices. Such events are mainly due to accidental coincidences from background radioactivity. Since the logic is also sensitive to relativistic particles, muons crossing at least seven planes also produce triggers. Usually these muons fire only the β-slices $+1$ and -1 but the coincidence of a muon with some radioactivity hits within a few microseconds can also fire different β-slices.

The analysis is based on the search for single space tracks in both wire and strip views and on the measurement of the velocity of the candidates. Due to the long time-of-flight of a slow monopole through the detector, the readout electronics must store streamer tube hits for ~ 500 μs. The width of such a temporal window is so large that on average three spurious hits are present in a 12×12 m^2 plane per event. With such a background, if we were to use only this tracking information, the probability of finding a fake track of ≥ 7 planes would be too high ($\sim 10^{-6}$) to carry out

a successful monopole search.

The ToF provided by the trigger allows further selection of the wire hits temporally compatible with the expected crossing time. In this way the effect of radioactivity background is considerably reduced and only a few hits are left for tracking. To reduce this background in the strip view, intersection with the selected wires is required. If a space track is found, a more refined time alignment searching for a track in the z–t temporal view (time track) is imposed. This technique has a strong rejection power against random time and spatial hit alignments due to radioactivity background: the probability of having an alignment in both spatial views and in the time view is negligible, $\sim 10^{-19}$ in the case of uncorrelated background. As a consequence, the main background is due to muons crossing at least seven horizontal planes combined with radioactivity noise which can simulate low β particles (the muon provides the spatial track while the noise confuses the time tracking algorithm).

A cut on the β of the track is performed to completely reject muons. Since muons survive all the analysis requirements but the β cut, they allow an estimate of the overall electronic and analysis efficiency by comparing the rate of reconstructed muons to the expected one. The efficiency of the time tracking algorithm and of the trigger circuits for slow particles has been evaluated and is taken into account in our overall efficiency (see Section 4.2).

3.2. Vertical trigger: slow particles

As in the previous case, the analysis is based on the search for associated space and time tracks. The hit selection procedure, however, is different because the trigger does not provide a ToF measurement: a track is required on the wires matching the pattern of fired vertical segments recorded in the trigger registers. This tracking requirement strongly reduces the uncorrelated background.

The time hits corresponding to spatial points on the track are used to get a rough estimate of the ToF. It is then possible to select the hits compatible with the measured ToF from the hit horizontal planes. Using these points, a final tracking is performed to reject accidental alignments, leaving only the muon background. On the basis of the measured velocity, slow monopole candidates are selected. Also in this case the efficiency can be evaluated by the analysis of the muons present in the sample of events.

3.3. Fast monopole analysis

The analysis strategy for fast monopoles is based on their expected high energy loss [13]. In particular monopoles with $\beta > 10^{-3}$ should produce a streamer charge several times higher than the one produced by a minimum ionizing particle with the same trajectory. Since the slow analysis covers the velocity range $\beta < 5 \times 10^{-3}$, a reasonable overlap is guaranteed with the fast analysis.

Events with a reconstructed track in both spatial (wire and strip) and temporal views, not recognized as slow monopole candidates from the previous analysis, are processed by the fast analysis.

In order to more completely understand the detector, several studies have been performed on the variation of streamer charge produced by muons as a function of gas mixture, high voltage and geometry of the track inside the tube. The streamer charge produced in each cell has been continuously monitored as a function of the length of the muon track projected along the wire direction (l_{proj}). In this way the contribution to the charge from geometrical factors and from small long term variations of the gas pressure and composition can be properly evaluated. Data show that for each l_{proj} interval, the charge distribution is gaussian with $\sigma/Q_{mean} \sim 30\%$. In Fig. 5 the average charge of the track $\langle Q \rangle$ is shown as a function of l_{proj} for a sample of tracks. An obscuration length [14] of ~ 1.3 cm can be inferred from the data. For l_{proj} shorter than the obscuration length the value of the charge is almost constant at the value Q_0. For greater l_{proj} the charge depends linearly on l_{proj}: $\langle Q(l_{proj}) \rangle = Q_0 + S \times l_{proj}$. The slope S has been studied as a function of the charge Q_0 measured for vertical incoming muons (Fig. 6), with Q_0 variations obtained by changing both the He/n-pentane ratio and the streamer tube high voltage. These results allow a prediction of the streamer charge for any monopole trajectory. As an example the streamer charge as a function of l_{proj} has been simulated for monopoles with $\beta = 5 \times 10^{-3}$ for which Q_0 is about four times higher than that produced by a vertical muon.

Since the charge is collected from the sum of several wire signals, particular care has been taken in handling

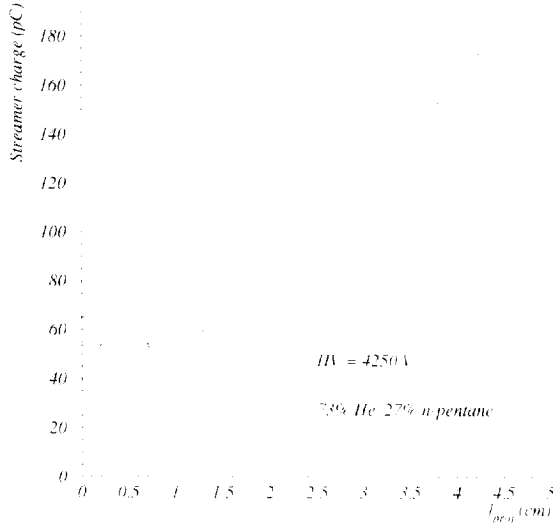

Fig. 5. Average streamer charge $\langle Q \rangle$ as a function of projected track length measured with muons. The first region is characterized by a constant value Q_0 of the charge ($\simeq 55$ pC) for l_{proj} smaller than ~ 1.4 cm (obscuration length); in the second region ($l_{proj} \geq 1.4$ cm) a linear increase is clearly observed.

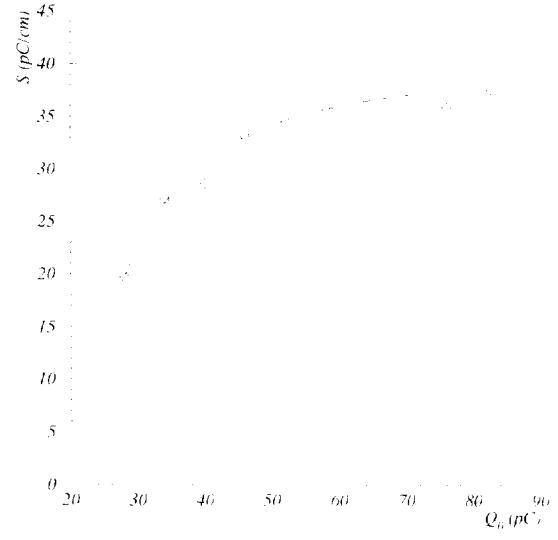

Fig. 6. Dependence of the slope S of the second region of Fig. 5 on the constant value Q_0 of the first region. The different Q_0 values have been obtained for different He/n-pentane ratios in the gas mixture and for different HV.

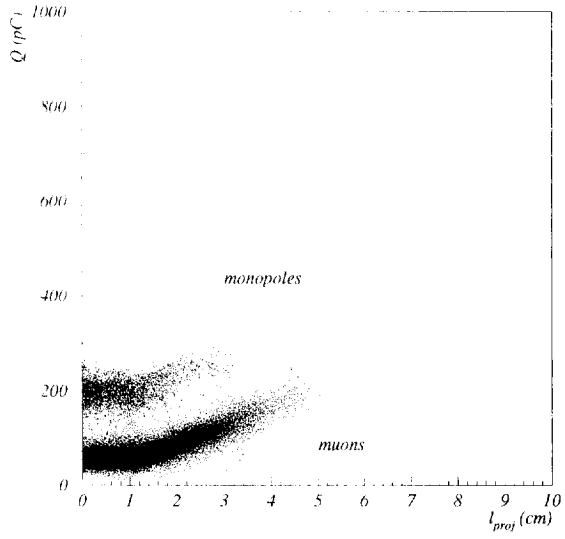

Fig. 7. Mean charge for a sample of muons and for simulated monopoles as a function of projected track length. A cut can be applied to discriminate monopoles with $\beta > 5 \times 10^{-3}$ with high efficiency and a small muon contamination.

events in which more than one wire has fired in one plane. In fact, due to time jitter, the streamers produced by a particle in a cluster of two or more adjacent wires can be observed either as a single pulse carrying the total charge or as multiple pulses. In the latter case the response of the charge readout electronics is affected by the recovery time of the charge integrator which is not easily monitored.

The main background is due to muon-induced showers that can produce high charges in some planes. This background can be reduced by computing the mean charge along the track without considering the highest value. Fig. 7 shows this mean charge versus l_{proj} for a sample of data as well as the expected monopole distribution obtained from the previous simulation. A further reduction of the shower background can be achieved on the basis of event topology. The surviving few tens of candidates per year will be analyzed in both the scintillator and track-etch sub-systems for a confirmation. Although the analysis procedures are well defined, more detailed studies of the streamer charge, including all the aforementioned effects, are in progress. In the following we will consider only the slow analysis.

4. Details of the slow monopole analysis

As an application of the analysis procedures described in the previous section, two samples of data, collected from February 1992 to January 1993 with the horizontal streamer monopole trigger only, have been analysed. The performance of the background rejection criteria and of the efficiency measurement methods have been fully tested.

The first sample, including 262 days of running, was collected with the trigger operating on two lower supermodules only; the second had 80 days of operation on two thirds of the lower part of the detector.

For this data the trigger rate was stable at ~ 80 triggers/hour per trigger unit. Some reductions were observed during short periods due to electronic failures or small variations of the streamer gas composition. Such effects have been taken into account in the efficiency estimate (see Section 4.2). Only a few runs were excluded from the analysis because of serious hardware problems: 6085 hours of live time survive the run cut ($\simeq 75\%$ of the solar time) during which 2.2×10^6 triggers were recorded.

The distribution of the fired β-slices in the first sample is shown in Fig. 3 for events firing at least one β-slice other than +1 and 1. The central peak is due to muon events in which some uncorrelated background hits simulated a longer ToF; the flatness of the distribution of the other slices guarantees the uniformity of trigger efficiency for particles of different β. The number of entries for each bin is consistent with the one expected from the uncorrelated radioactivity background (see Section 2.3).

4.1. Analysis procedure

The analysis procedure starts from the measure of the ToF of the particle provided by the trigger. Since several β-slices may be fired in the same event, the analysis procedure described below is performed for each of the fired β-slices.

- The first step is the selection of the streamer tube hits, recorded in the QTP memory, compatible with the fired slice: for each plane the hits within $\pm 10\ \mu$s from the expected crossing time of the monopole, as calculated from the β-slice value, are selected. The width of this window has been determined by a Monte Carlo study to ensure nearly 100% collection efficiency.
- For each of the selected hits a match is required between the wire coordinate and the coordinate (1 m resolution) provided by the QTPs. To increase efficiency, if no QTP hits are present at any time corresponding with a given wire hit, the hit is preserved. This procedure reduces the radioactivity background hits present in the slow readout chain by a factor ~ 20 and greatly simplifies tracking. In particular short fake tracks due to accidental alignments of spurious hits are removed.
- Since we do not expect multiple monopoles in one event, a single track is required, firing at least seven planes.
- If wire tracking is successful, we analyze the second spatial view of the event given by the strips. Since they have no associated time information, a different background suppression procedure is adopted: for each module only the strips that intersect wires which fired within the time window are selected.
- A track is looked for in the strip view. In order to reduce the effect of possible inefficiencies only six hits are required to be aligned.
- A more refined time alignment than the one selected at the trigger level is required by searching for a track in the QTP time view. The used resolution is derived from the ~ 600 ns maximum time jitter. Time hits are required to be consistent with the wire hits used in the wire tracks. Moreover, in order to improve the time resolution of the algorithm, time hits due to possible afterpulses in the streamer tubes are suppressed: those within 750 ns from the previous hit on the same QTP channel are not included in the tracking.
- Time tracking requires at least seven planes; if more than one track is present, the one with the greatest number of planes is used.

The β distribution of the 1.1×10^6 events that survive the requirements is shown in Fig. 8. Monopole candidates were further required to have $\beta < 5 \times 10^{-3}$.

After these cuts no events survive. The events rejected here will be further processed by the fast analysis, since charge information provides a more powerful tool to tag fast monopoles in the excluded β region.

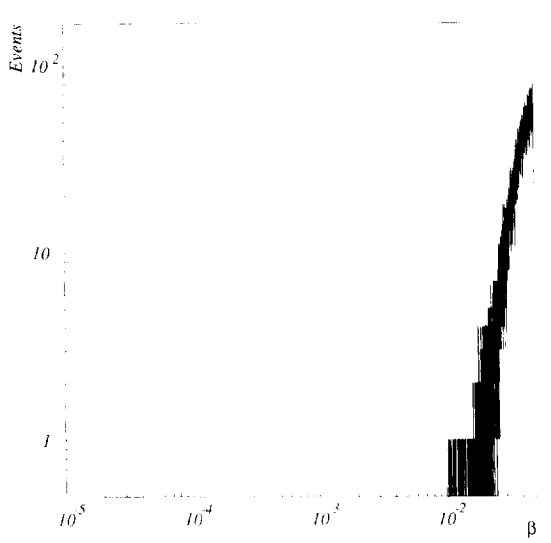

Fig. 8. Beta distribution for reconstructed events: only the β region relevant for this analysis is shown. No events are present in the $\beta < 10^{-2}$ region.

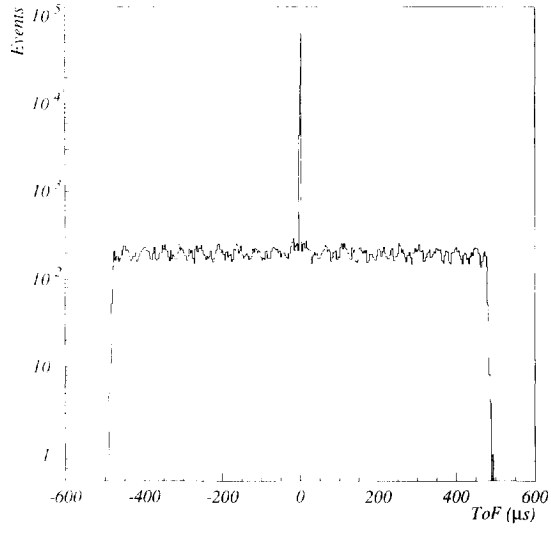

Fig. 9. ToF distribution for the same data of Fig. 3. The periodic structure and the central peak of Fig. 3 are still evident. The flatness of the distribution ensures the independence of the analysis on β.

4.2. Efficiency measurement and flux limit

The 90% confidence level upper limit for an isotropic monopole flux is given by the following expression:

$$\Phi_M \leq \frac{2.3}{\int\int \frac{dA(\theta,\phi,t)}{d\Omega}\varepsilon(\theta,\phi,t)\,d\Omega dt}$$

where $dA(\theta,\phi,t)/d\Omega$ is the differential acceptance obtained by a Monte Carlo simulation which includes all the geometrical and trigger requirements and $\varepsilon(\theta,\phi,t)$ is the overall efficiency as a function of the the zenith angle θ and of the azimuth ϕ.

In our case the sensitivity of the horizontal monopole trigger to muons provides a simple way to estimate the overall efficiency $\varepsilon(\theta,\phi,t)$; in fact muons crossing at least seven planes survive all the analysis steps but the cut on β. There are, however, two possible sources of unaccounted inefficiencies because muons concentrate in the region around $\beta = 1$.

1. Failure of the time tracking algorithm. The performance of the time tracking algorithm for slow particles has been checked by applying the time tracking to the sample of events in Fig. 3 without imposing any spatial requirement. Fig. 9 shows the distribution of the reconstructed time of flight. The response of the algorithm is flat and the fraction of reconstructed events, $\simeq 69\%$, is expected from the different time resolution of the β-slices and of the tracking algorithm. This implies that the analysis efficiency $\varepsilon_a(\theta,\phi,t)$ measured with muons is independent of β and is representative of the efficiency at any velocity.
2. Failure of the trigger circuitry. To take into account the possible effects on the detection of slow particles due to trigger inefficiency, electronic failures and the fraction of the eleven trigger units actually operating, we include the efficiency term $\varepsilon_e(t)$.

Since the $\varepsilon_a(\theta,\phi,t)$ and $\varepsilon_e(t)$ contributions are not completely independent (some of the possible trigger failures affect muon detection as well) the overall efficiency can be underestimated by

$$\varepsilon(\theta,\phi,t) = \varepsilon_a(\theta,\phi,t) \times \varepsilon_e(t).$$

The first contribution is estimated by computing the ratio of the rate of single muons reconstructed by this analysis to the expected rate of single muons crossing at least seven horizontal planes. This expected rate is estimated from the results of a completely independent analysis performed on muons observed when the entire lower part of the apparatus was running; the effect of possible inefficiencies has been reduced by also

accepting tracks with less than seven fired planes. The average analysis efficiency $\langle \varepsilon_a \rangle$ in the data sample is over 90%.

Since the angular distribution of monopoles is expected to be different from the one for muons, the efficiency has been computed as a function of θ and ϕ. However, from the data we infer that it is independent of θ and ϕ, so we consider $\varepsilon_a(\theta, \phi, t) = \varepsilon_a(t)$.

The second contribution is evaluated by monitoring the ratio of the measured rate to the one expected on the basis of the observed background single wire hit rate (see Sec. 2.3) through the whole data taking period, for each trigger unit and for each β-slice. Moreover, at the end of each run an automatic test procedure checks the correct operation of all horizontal trigger circuits. The measured trigger efficiency is over 99%.

Taking into account all the aforementioned effects, for $1.1 \times 10^{-4} < \beta \leq 5 \times 10^{-3}$ we have

$$\Phi_M \leq \frac{2.3}{A_1 \int_0^{t_1} \varepsilon(t)\,dt + A_2 \int_0^{t_2} \varepsilon(t)\,dt} \simeq 8.9 \times 10^{-15}\ \mathrm{cm^{-2}\ s^{-1}\ sr^{-1}}$$

where $A_1 = \int (dA(\theta, \phi)/d\Omega)\,d\Omega = 1390\ \mathrm{m^2\ sr}$ is the acceptance of the two lower supermodules running for $t_1 = 4645$ live time hours (first sample) and $A_2 = \int (dA(\theta, \phi)/d\Omega)\,d\Omega = 2830\ \mathrm{m^2\ sr}$ is the acceptance of the four lower supermodules running for $t_2 = 1086$ live time hours (second sample). The acceptances take into account the horizontal trigger requirements, and the total live time has been corrected for dead time.

5. Conclusions

We have described the analysis procedures that will be adopted in the monopole search performed with the streamer tube sub-system of the MACRO detector. We have applied this procedure to a sample of data collected with the horizontal streamer tube monopole trigger. The results yield a 90% confidence level upper limit to the flux of bare monopoles with $1.1 \times 10^{-4} < \beta \leq 5 \times 10^{-3}$ of $8.9 \times 10^{-15}\ \mathrm{cm^{-2}\ s^{-1}\ sr^{-1}}$. Although the data discussed here represent only a small fraction of the expected final MACRO statistics, this result is already comparable with the best limit obtained with any other helium filled gas detector [15].

Acknowledgements

We gratefully acknowledge the support of the director and of the staff of the Laboratori Nazionali del Gran Sasso and the invaluable assistance of the technical staff of the Institutions participating in the experiment. We thank the Istituto Nazionale di Fisica Nucleare (INFN), the U.S. Department of Energy, and the U.S. National Science Foundation for their generous support of the MACRO experiment. We thank INFN for providing fellowships and grants (FAI) for non Italian citizens.

References

[1] M.S. Turner et al., Phys. Rev. D 26 (1982) 1296.
[2] S. Ahlen et al., Phys. Rev. Lett. 72 (1994) 608.
[3] S. Ahlen et al., Nucl. Instr. Meth. A 324 (1993) 337.
[4] MACRO proposal Servizio Documentazione Laboratori Nazionali di Frascati November 1984.
[5] S. D. Drell et al., Phys. Rev. Lett. 50 (1983) 644.
V. Patera, Phys. Lett. A 137 (1989) 259.
[6] G. Battistoni et al., Nucl. Instr. Meth. A 235 (1985) 91.
[7] L. Bracci et al., Phys. Lett. B 124 (1983) 493; B 143 (1984) 357.
[8] G. Battistoni et al., Nucl. Instr. Meth. A 270 (1988) 185.
[9] M. Ambrosio et al., Nucl. Instr. Meth. A 321 (1992) 609.
[10] Produced by CAEN, Viareggio, Italy.
[11] V.A. Rubakov, JETP Lett. 33 (1981) 644.
C.G. Callan, Phys. Rev. D26 (1982) 2058.
[12] G. Auriemma et al., Nucl. Instr. Meth. A 263 (1988) 249.
[13] S. Ahlen in "Magnetic Monopoles" NATO ASI series, Series B: Phys. Vol. 2, Plenum Press, N.Y. (1982).
[14] E. Iarocci, Nucl. Instr. Meth. 217 (1983) 30.
[15] K.N. Buckland et al., Phys. Rev. D 41 (1990) 2726.